Table 4.6 Details of borehole investigations (AN-1, 3)

	AN-1	AN-3
Depth (m)	1,000	408
Diameter	HQ (about 100 mm)	HQ (about 100 mm)
Drilling fluid	Fresh water	Fresh water
Geophysical logging*	○	○
BTV investigations	○	○
In-hole hydraulic test	(33 intervals)	(24 intervals)
Laboratory tests using rock specimen	Apparent density (20 samples) Effective porosity (20 samples) Water content (20 samples) Seismic wave velocity (20 samples) Uniaxial compression test (20 samples) Brazilian test (40 samples)	—
Hydraulic fracturing test	(20 samples)	—

* : Electrical, Micro resistivity, Density, Neutron, Gamma-ray, Acoustic, Temperature, Caliper and Deviation

4.1.3 Geological results - results of Phase I-a

Phase I-a includes the work for the MIU Project at the Shobasama Site. This includes the entire borehole drilling at the site in the reporting period (1996-1999), all the multi-disciplinary borehole investigations and any surface investigations such as the geophysical surveying. Lastly, it includes any modeling based on the new information developed in the period.

In Phase I-a, EM magnetotelluric and reflection seismic surveys were done, three boreholes were drilled (MIU-1, 2 and 3, Table 3.2) and multidisciplinary borehole investigations were carried out at the Shobasama Site. Based on the results of these investigations, a revised geological model was constructed. Details of the investigations are as follows.

4.1.3.1 Magnetotelluric survey

A resistivity survey was carried out at the Shobasama Site (survey line: N-S, 200 m, Table 3.1). However, accurate results were not obtained because of the low-resistivity zone in the near-surface part of the site. Also, application testing of a remote-reference method in magneto electric survey (MT) was carried out aiming at understanding the geological structure in deeper parts of the site. The remote- reference method takes advantage of high coherency of MT signal compared with that of regional noise. By comparing the measurement data at two locations, the MT signal can be separated from the regional noise. Unfortunately, reliable data was not obtained because of excessively high noise levels. Thus the results of these surveys are not presented in this report.

4.1.3.2 Reflection seismic survey [37,38]

A reflection seismic survey was carried out to obtain data on geological structures of Mizunami Group and the depth and geometry of unconformity between the basal conglomerate and the Toki granite. Survey lines were run N-S and E-W and are shown in Figures 4.4 and 4.9. These data are used to construct the geological model. Details of the reflection seismic survey are shown in Table 4.7.

Some continuous reflection planes are detected above an elevation of 100 masl throughout both survey lines. The reflectors are consistent with the shape of unconformity between the sedimentary rocks and the basement granite and the internal structures of the sedimentary rocks (Figure 4.10). While partial discontinuities (SF-1-3 in Figure 4.10) are recognized, it was not confirmed whether or not they represent faults.

The reliability of the results below a depth of 200 m was reduced because the survey lines were not long enough and the presence of strong reflections in both the sedimentary rocks and the upper part of the granite.

Table 4.7 Details of reflection seismic survey

Reflection Seismic survey (See Figure 4.4 and 4.9)	Line-3-1 (650 m)	・Seismic source : dynamite ・Seismic source interval : 5m ・Receiver interval : 5m ・Sampling rate : msec ・Data length (Recording time): 2s
	Line-3-2 (600 m)	・Seismic source: Dropped weight, vibrator ・Seismic source interval : 5m ・Receiver interval : 5m ・Sampling rate : 1msec ・Data length (Recording time): 2s

4.1.3.3 MIU series 1, 2 and 3 borehole investigations (39~41)

Borehole investigations are one of the most important methods to investigate the underground geology and geological structure prior to excavation. These investigations allow collection of core samples, groundwater sampling and measuring the hydrogeological and rock mass properties to depth.

In Phase I-a, geological studies included detailed core logging, borehole geophysics and BTV surveys in the three new 1,000 m-deep boreholes, MIU-1, 2 and 3. Furthermore, petrological and mineralogical studies were carried out using core samples from the boreholes.

Core descriptions include: drilling depth, lithology, rock name, textural description such as grain-size and fabric, mafic mineral content, color, weathering, alteration, RQD, core recovery rate, fracture shape, fracture type and mineral fillings.

Borehole geophysical surveying includes a variety of methods: electrical logging, micro-resistivity logging, density logging, neutron and gamma-ray logging, acoustic logging, temperature logging, caliper logging and borehole deviation surveying. In addition, Borehole TV investigations record images of features, especially structures along a borehole wall. The records include depth, shape, width, fracture aperture, presence of filling and possibly alteration. Orientations are calculated from the geometry of features observed in the boreholes.

For petrological and mineralogical studies, modal and chemical composition analyses are carried out.

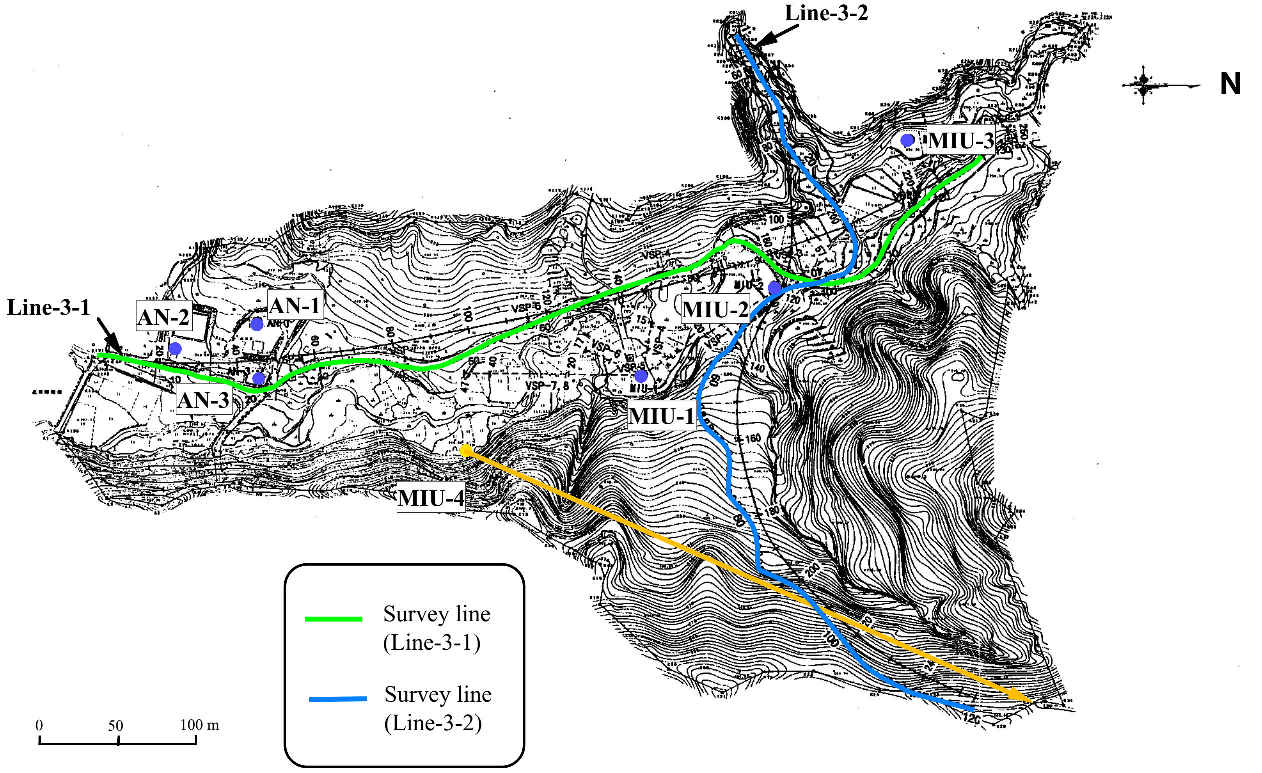

Figure 4.9 Location map of the survey line in Shobasama Site for reflection seismic survey

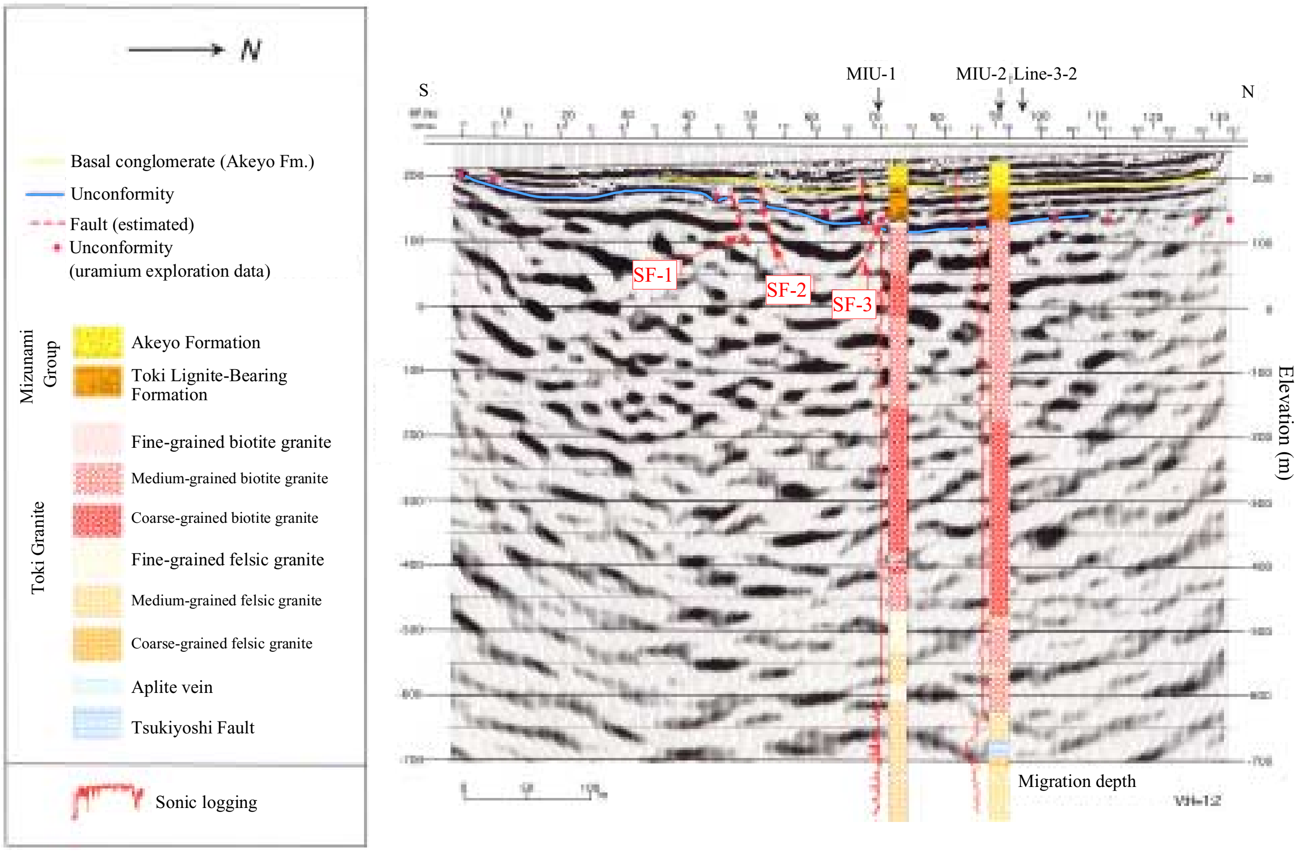

Figure 4.10 Results of reflection seismic survey (Line-3-1)

The results of the above investigations, the core descriptions, geophysical logging, BTV investigations and petrological and mineralogical studies in MIU-1, 2 and 3 are described below. In addition, overviews of the results from these boreholes are shown in Appendices 1, 2 and 3.

Granite lithofacies

Based on the core recovered from the MIU-1, 2 and 3 boreholes, the granite in the Shobasama Site has been classified into 'Biotite granite' and 'Felsic granite' phases. Furthermore, the biotite granite is subdivided into coarse-grained, medium-grained and fine-grained textural types.

The modal analysis of core samples from MIU-1, 2 and 3 indicate the rocks intersected are true granites (Figure 4.11) as classified by the IUGS (1973).

According to the chemical composition analyses, the chemical compositions of the biotite granite and felsic granite phases, in terms of some major oxides are different. An analysis of the variation in major oxide content versus depth, using a least-squares approximation, shows that the trends are different for most oxides in the two rock types. The analyses plot along different lines on the major oxide content-vs. depth diagrams (Figure 4.12).

Characteristics of the fracture distributions in the granite

In MIU-1, 2 and 3, sedimentary rocks were intersected from the surface to approximately 88 to 89 m depth, and these unconformably overly the biotite granite. The uppermost part of the granite is a strongly weathered, approximately 15 m thick zone.

Figure 4.13 shows changes in fracture density, cumulative fracture frequency, and orientation of fractures with depth in the MIU-2. Figure 4.14 shows histograms of fracture frequency distributions related to depth. Based on the variations shown in fracture density and by the cumulative fracture frequency analysis, the granite can be divided into the following three structural domains: "Upper fracture zone", "Moderately fractured zone" and "Fracture zone along the fault" in descending order. Characteristics of each domain are as follows.

・**"Upper fracture zone"**

This zone ranges from the weathered top of the granite down to approximately 300-370 m depth in the three boreholes. The fracture density varies from 3 to 5 fractures per meter (Table 4.8). This zone is characterized by the prevalence of fractures with a shallow inclination (Figure 4.15, Table 4.8).

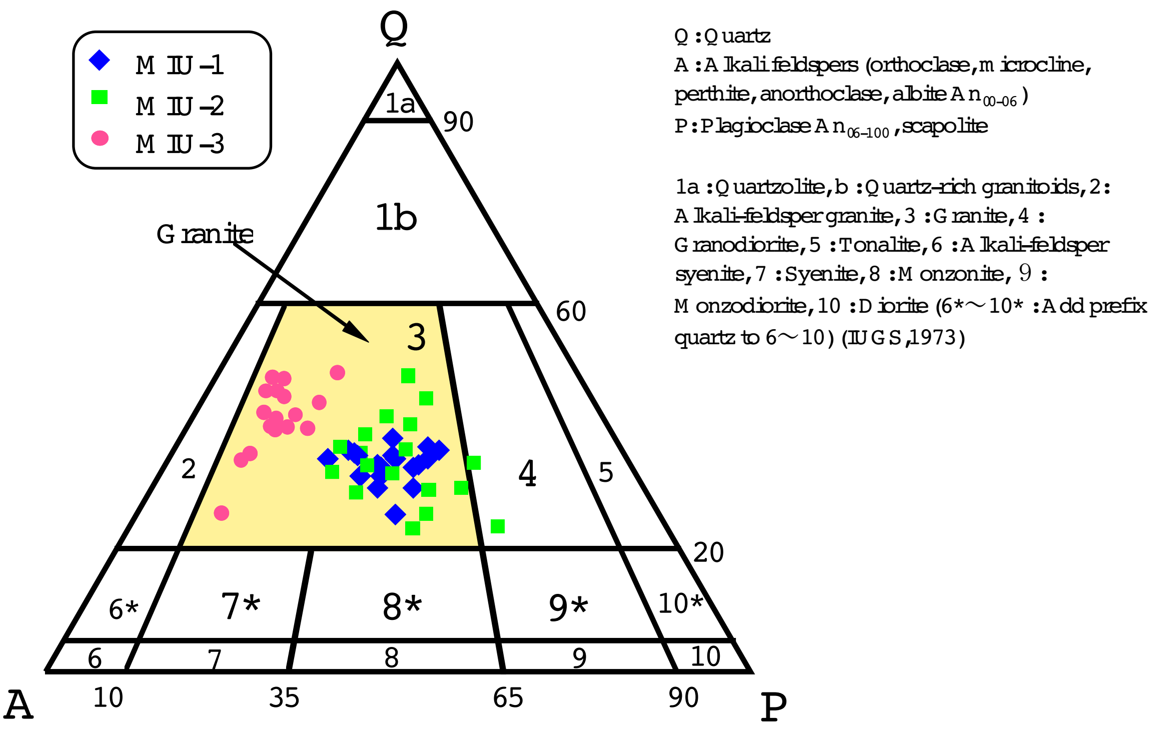

Figure 4.11 Modal composition of the Toki Granite

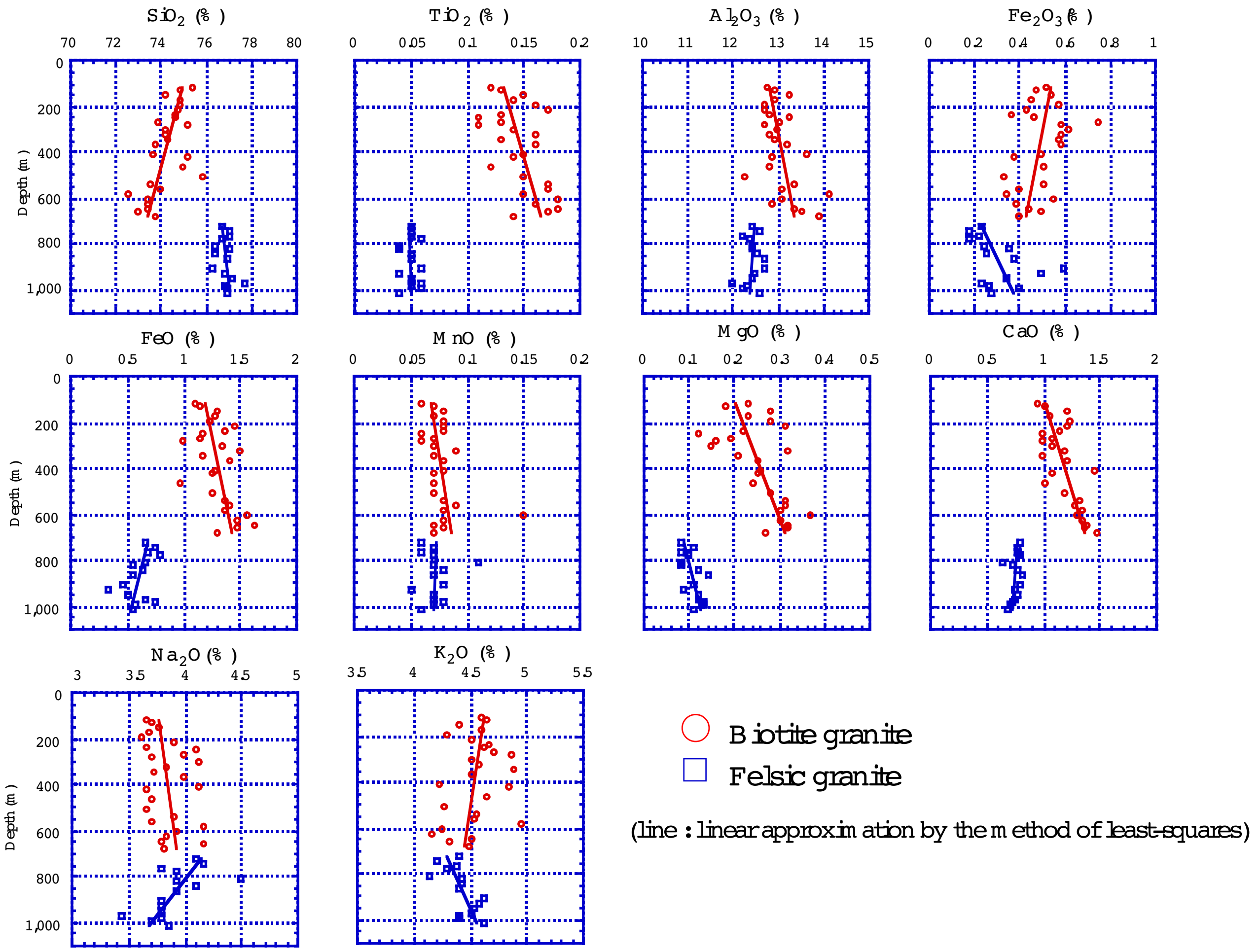

Figure 4.12 Chemical compositions of the Toki Granite

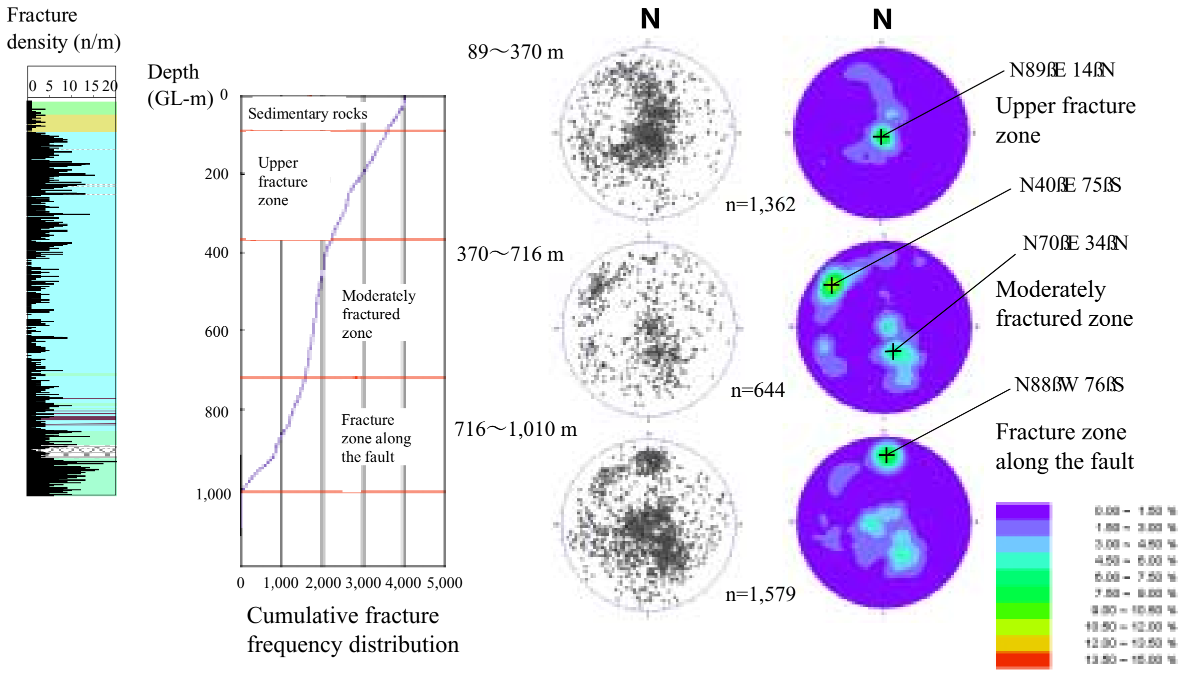

Figure 4.13 Fracture density, cumulative fracture frequency distribution and orientation of fractures vs depth (MIU-2)

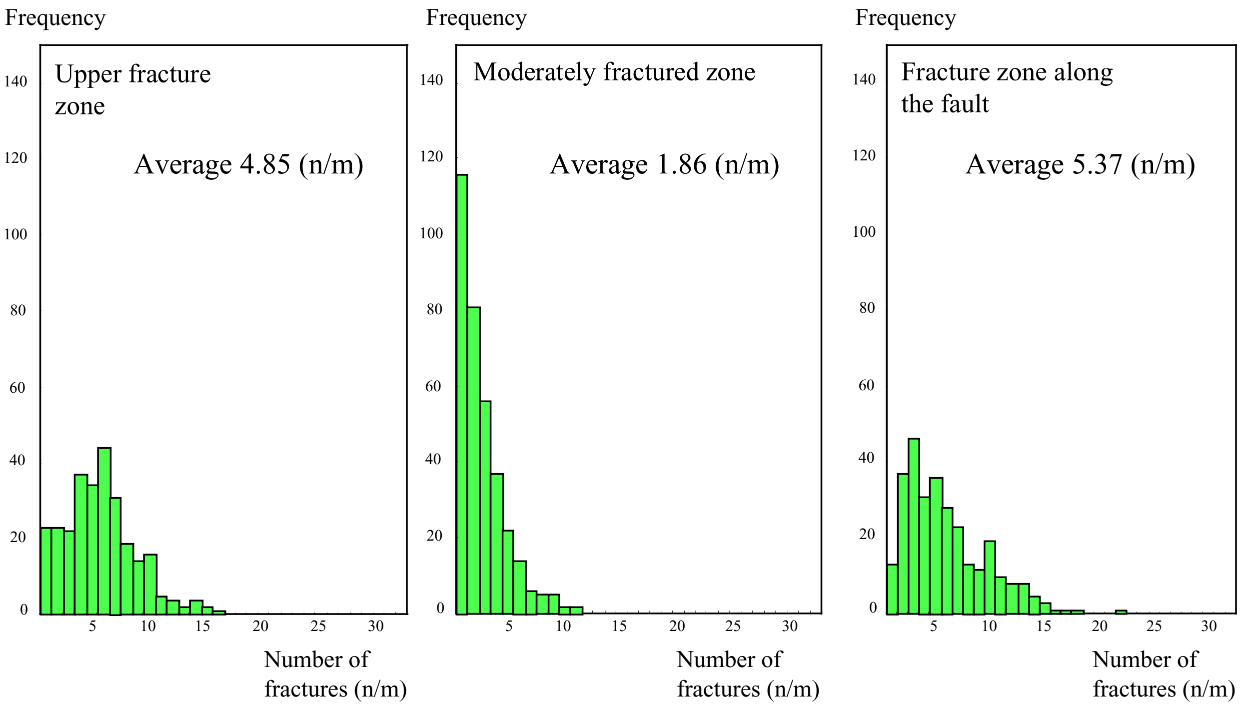

Figure 4.14 Fracture density vs depth (MIU-2)

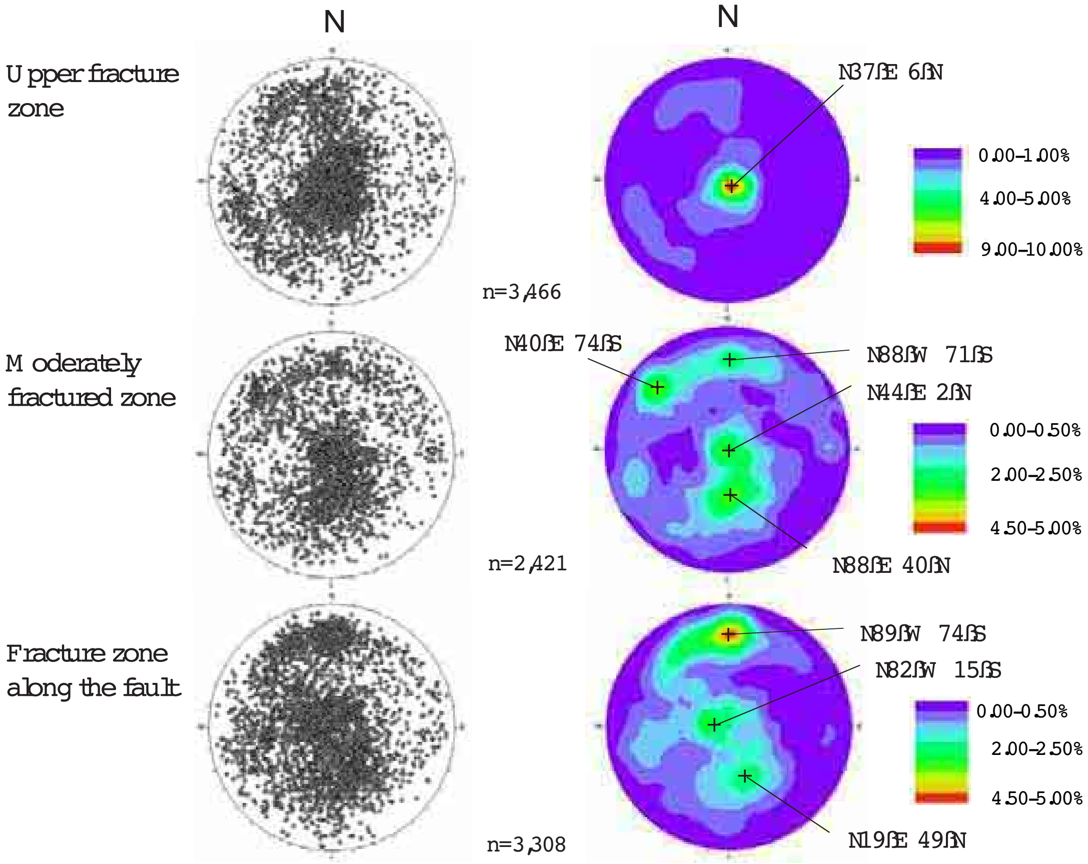

Figure 4.15 Orientation of fractures vs depth (MIU-1~3)

“Moderately fractured zone”

This zone occurs between the “Upper fracture zone” and the “Fracture zone along the fault”. The fracture frequency ranges, on average, from 1 to 3 fractures per meter in the three boreholes (Table 4.8). Like the underlying “Fracture zone along the fault”, this zone is composed of a combination of shallow (0-30 °), middle (30-60 °) (strike: E-W, dip: N) to high (60-90 °) (strike: NE-SW, dip: SE) -inclination fractures as shown in Figure 4.15 and Table 4.8.

・**“Fracture zone along the fault”**

This zone is characterized by the concentration of fractures developed along the Tsukiyoshi Fault, ranging in density from 3-6 fractures per meter in the three boreholes (Table 4.8). This zone is composed of low, middle (strike: NNE-SSW, dip: WNW) and high (strike: E-W, dip: S) -inclination fractures (Figure 4.15, Table 4.8). In particular, the strike of the most common fractures is approximately EW with steep southerly dips, which may be a reflection of the orientation of the Tsukiyoshi Fault.

Table 4.8 Densities and prevailing orientations of fracture in each structural domain

	“Upper fracture zone”	“Moderately fractured zone”	“Fracture zone along the fault”
Average fracture density*	3 to 5 /m	1 to 3 /m	3 to 6 /m
Prevailing orientations, Strike/dip	・Low/	・Low/ ・High/EW, S ・Medium/ EW, N ・High/ NE-SW, SE	・Low/ ・High/ EW, S ・Medium/ NNE-SSW, WNW

*：Fracture data obtained from the BTV investigations

In general, the “Upper fracture zone” and the “Fracture zone along the fault” are characterized by higher hydraulic conductivity (10^{-7} to 10^{-5} m/s) than the “Moderately fractured zone” with lower conductivities (10^{-7} to 10^{-10} m/s) (Figure 4.16).

Differences in fracture characteristics such as shapes and mineral fillings in the three structural domains are yet to be analyzed.

Physical properties obtained by borehole geophysics in the granite

In the MIU-1, 2 and 3 boreholes, geophysical surveys included:

・electrical logging
・micro-resistivity logging
・density logging
・neutron logging
・gamma-ray logging
・acoustic logging
・temperature logging
・caliper logging
・borehole deviation logging.

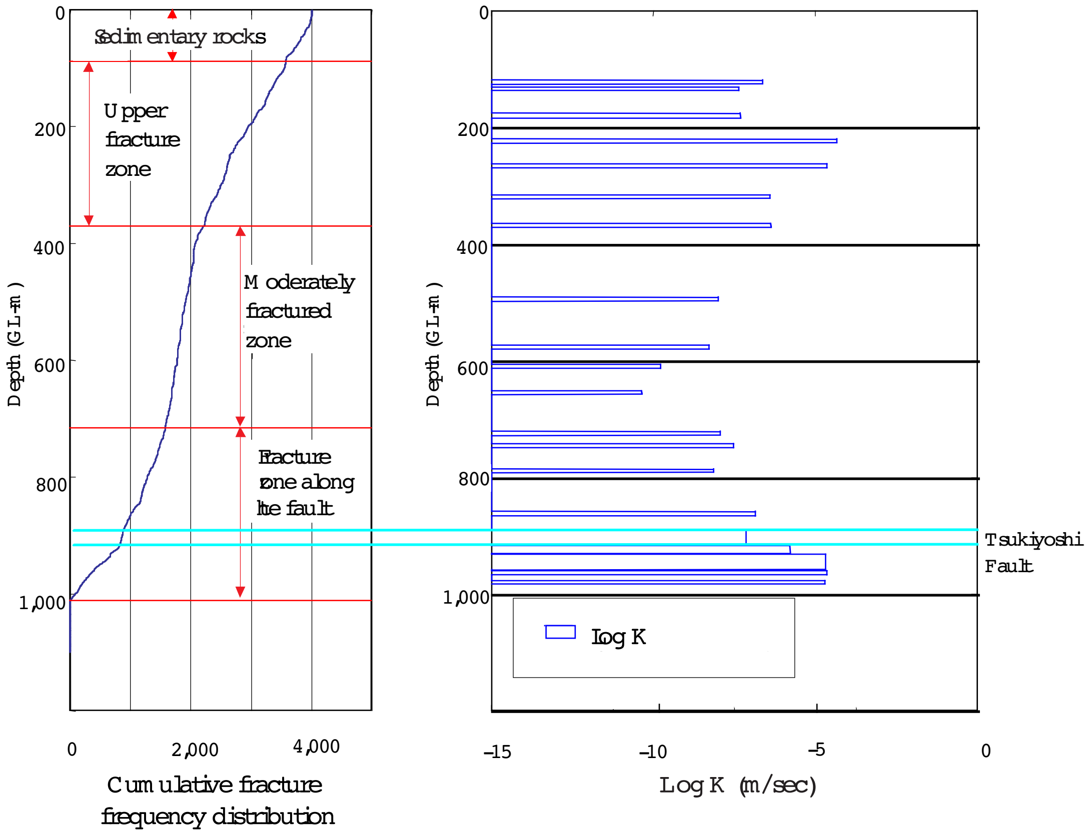

Figure 4.16 Comparison between cumulative fracture frequency distribution and hydraulic conductivity distribution

The results of the apparent resistivity (short and long-normal) obtained from electrical logging, porosity obtained from neutron logging and P-wave velocity obtained from acoustic logging are shown on Figure 4.17. Anomalies in the log profiles of these three methods are considered to provide good indications of increased permeability in the rock mass. Stated very simply, the two former methods give indications of water content and the latter can be an indication of the degree of fracturing of a rock mass. Neutron logging is based on the principal that neutrons are scattered or slowed by collisions with hydrogen atoms and gamma radiation produced. For our purposes, hydrogen is present only in water or in hydrated minerals. Thus an increase in water results in an increase in neutrons captured or moderated. Therefore, saturated rocks with high porosity will have a lower neutron count than low porosity rocks. With respect to electrical resistivity, the rocks and soils of the earth exhibit a wide range. The presence of water increases the ability of earth materials to conduct electricity. Therefore, very simply stated, unsaturated or slightly saturated rocks will normally have a higher resistivity than the same rocks under more saturated conditions. With respect to acoustic logging, the P-wave velocity, which is very dependent on rock type, will be faster in intact rock than in the same rock if it is fractured. As the degree of fracturing increases the P-wave velocity decreases. And as the degree of fracturing increases the permeability will also likely increase.

The results of comparison of porosity, apparent resistivity and P-wave velocity among the three zones of the granite are as follows.

・ Porosity

The range of average porosity of “Upper fracture zone”, “Moderately fractured zone” and “Fracture zone along the fault” determined by neutron logging are 4 to 7%, 3 to 5% and 4 to 8%, respectively. Intersections of the Tsukiyoshi Fault (highlighted by yellow in Figure 4.17) show porosities of about 8% and 14% respectively in MIU-2 and 3.

・ Apparent resistivity

The average apparent resistivity is smallest in the “Fracture zone along the fault” and largest in the “Moderately fractured zone”. The ranges of average resistivity in Ωm are:

- ”Upper fracture zone”: short-normal- 800 to 2,000; long-normal 1,800 to 2,800
- ”Moderately fractured zone”: short normal 1,500 to 2,500; Long normal 2,800 to 3,500
- ”Fracture zone along the fault”: short normal 400 to 1,500, long normal 700 to 1,600

Local decreases in apparent resistivity occur at shorter intervals in the ‘”Upper fracture zone” than in the “Moderately fractured zone”. The average apparent resistivities of the Tsukiyoshi Fault measured in MIU boreholes are very low:

MIU-2: short normal 400 Ωm, long normal 300 Ωm

MIU-3: short normal 100 Ωm, long normal 200 Ωm

・P-wave velocity

The smallest average P-wave velocity is obtained in the “Fracture zone along the fault” and largest in the “Moderately fractured zone”. The ranges are:

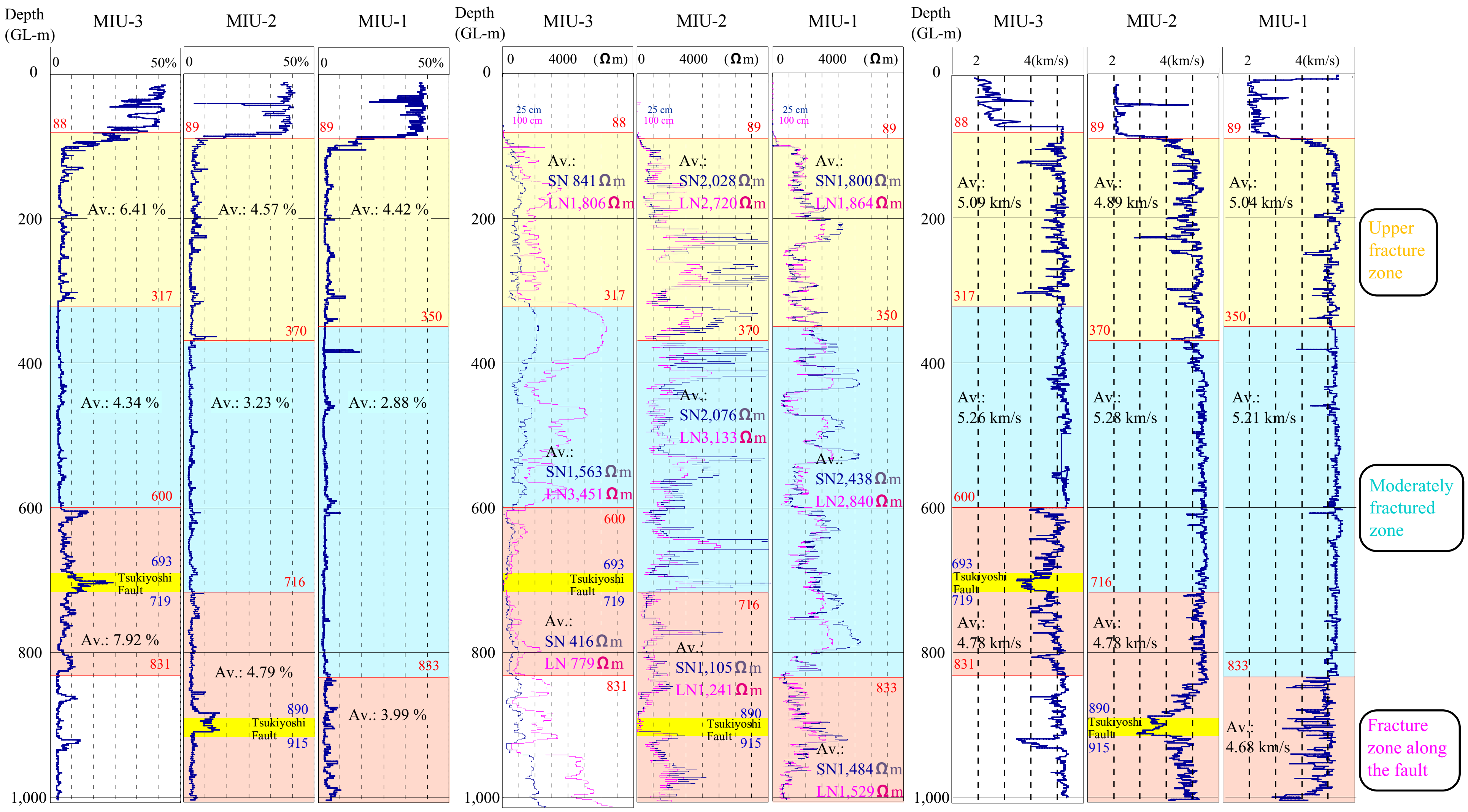

(a) Neutron porosity (b) Apparent resistivity (c) P-wave velocity

SN : short normal (25 cm)
LN : long normal (100 cm)

Figure 4.17 Results of geophysical logging

'Upper fracture zone', 'Moderately fractured zone' and 'Fracture zone along the fault' are defined according to the result of fracture density and geophysical logging.

“Upper fracture zone” 4.8 to 5.1 km/s
“Moderately fractured zone” 5.2 to 5.3 km/s
“Fracture zone along the fault” 4.6 to 4.8 km/s

Local decreases in P-wave velocity (<5.0 km/s) appear more often in the “Upper fracture zone” than in the “Moderately fractured zone”. P-wave velocity averages in the Tsukiyoshi Fault are lower than 0.4 km/s in MIU-2, 3.

Characteristics of faults in the granite

The Tsukiyoshi Fault is intersected by MIU-2 at 890 to 915 m depth and by MIU-3 at 693 to 719 m depth. In both intersections the core of the fault is composed of about a 10 to 20 m-wide cataclasite zone around which an approximately100 m-wide fractured zone is developed. In particular the “Fracture zone along the fault” intersected by MIU-2 is much more permeable than the “Moderately fractured zone” (Figure 4.16).

4.1.4 Construction of the geological model for the about 4 km × about 6 km study area

4.1.4.1 Conceptualization of the geological model for the about 4 km × about 6 km study area surrounding the Shobasama Site : data from the literature and “other geoscientific research”

Geological units

The geological model was constructed solely with data from the literature and the “other geoscientific research” for the about 4 km × about 6 km study area (Figure 3.4).

For both sedimentary rocks and granite, lithofacies are considered as primary whereas fractures and faults are secondary features generated after rock formation.

The following sedimentary rocks are treated as individual units in the geological model: the Seto Group, and the Oidawara, Akeyo and Toki Lignite-bearing Formations. For granite, it is divided into only two parts; the upper highly weathered zone is considered as a separate geological component from the rest of the granite below the weathered zone. The Tsukiyoshi Fault is a structural part of the model that crosscuts the lithological units.

Model construction

Using the data from the sources shown in Table 4.9, the geological units and their physical boundaries were defined. Topographical features, each unit’s boundary and the shape of the fault plane were estimated using the minimum tension theory [42] (Figure 4.18). The results of borehole investigations in AN-1 and 3 were used to extract the geological units. However, these results were not used when defining the above-mentioned boundaries as the granite was only divided into three parts in these boreholes: weathered granite, the granite below the weathered zone and the Tsukiyoshi Fault.

Table 4.9 Sources of data used to define geological structural boundaries of the geological model
(Study area: about 4 km×about 6 km)
(MIU Phase I-a sources are excluded)

Boundary	Data Source
Ground surface	Digital elevation data (20 m mesh)*
Upper boundary of Oidawara Fm.	59 boreholes for uranium exploration AN-8, SN-1, 2, 3 and 4, TH-6, 8 Seismic survey in the Shaft Excavation Effect Experiment*
Upper boundary of Akeyo Fm.	53 boreholes for uranium exploration AN-8, SN-1, 2, 3 and 4,TH-6, 8 Geological map (PNC, 1994)
Upper boundary of Toki Lignite-bearing Fm.(Upper)	135 boreholes for uranium exploration AN-6, 8, SN-1, 2, 3, 4 and 6,TH-1, 2, 3, 4, 6, 7 and 8 Seismic survey in the Shaft Excavation Effect Experiment*
Upper boundary of Toki Lignite-bearing Fm.(Lower)	141 boreholes for uranium exploration AN-6, 8,SN-1, 2, 3, 4 and 6,TH-1, 2, 3, 4, 6, 7 and 8 Seismic survey in the Shaft Excavation Effect Experiment*
Upper boundary of weathered granite	120 boreholes for uranium exploration AN-6, 8, SN-2, 3, 4 and 6, TH-1, 2, 3, 5, 7, 8, HN-1 Topographical map of basement rock (20,31) Seismic survey in the Shaft Excavation Effect Experiment*
Upper boundary of intact granite	(Calculated by assuming the thickness of weathered granite is 20 m)
Tsukiyoshi Fault	13 boreholes for uranium exploration TH-1, 2 and 3 Topographical map of basement rock (31) Seismic survey in the Shaft Excavation Effect Experiment*

*：1:25,000 “Toki” and “Mizunami” topographic maps published by Geophysical Survey Institute

As with most models, there are uncertainties. The main ones are considered to be as follows:

① Data on the heterogeneity of the granite deep underground were scarce. As a result, the granite could only be divided into two units: the weathered zone at the top and the rest of the granite.
② Information on the Tsukiyoshi Fault was not available where it crosscuts the granite. Thus, it was postulated that the fault in the granite has the same properties as it has in the sedimentary rocks.

4.1.4.2 Revision of the geological model with data from MIU Phase I-a

The initial geological model was revised with data from the MIU Phase I-a

Geological units

For the sedimentary rocks, the Seto Group, and the Oidawara, Akeyo and Upper and Lower Toki Lignite-bearing Formations there was no change in these geological units.

For the granite, the weathered zone remained the same. The previously undivided granite could be subdivided on a structural basis into domains, the: “Upper fracture zone”, “Moderately fractured zone” and

"Fracture zone along the fault". The Tsukiyoshi Fault was included as before.

Model construction

Using the data from the sources shown in Table 4.10, the boundaries between the above geological units were defined. The drilling results of AN-1 are also included in the data.

Table 4.10 Data sources used to set geological boundaries of the geological model
(Study area : about 4 km×about 6 km)
(MIU Phase I-a sources included)

Boundary	Data Source	
	Data obtained by literature study / geoscientific research prior to the MIU Project	MIU Project data Phase I-a
Ground surface	Digital elevation data (20 m mesh)*	—
Upper boundary of Oidawara Fm.	59 boreholes for uranium exploration AN-8, SN-1, 2, 3 and 4, TH-6, 8 Seismic survey in the Shaft Excavation Effect Experiment*	—
Upper boundary of Akeyo Fm.	53 boreholes for uranium exploration AN-8, SN-1, 2, 3 and 4, TH-6, 8 Geological map (PNC, 1994)	—
Upper boundary of Toki Lignite-bearing Fm. (Upper)	135 boreholes for uranium exploration AN-6, 8, SN-1, 2, 3, 4 and 6,TH-1, 2, 3, 4, 6 and 8 Seismic survey in the Shaft Excavation Effect Experiment*	—
Upper boundary of Toki Lignite-bearing Fm. (Lower)	141 boreholes for uranium exploration AN-6, 8, SN-1, 2, 3, 4 and 6, TH-1, 2, 3, 4, 6 and 8 Seismic survey in the Shaft Excavation Effect Experiment*	—
Upper boundary of weathered granite	120 boreholes for uranium exploration AN-6, 8, SN-2, 3, 4 and 6, TH-1, 2, 3, 4, 5, 7 and 8, HN-1 Topographical map of basement rock(20,31) Seismic survey in the Shaft Excavation Effect Experiment*	—
Upper boundary of "Upper fracture zone"	**AN-1 (34)**	**MIU-1, 2 and 3 (39～41)**
Upper boundary of "Moderately fracture zone"	**AN-1 (34)**	**MIU-1, 2 and 3 (39～41)**
Tsukiyoshi Fault	**Geological map (12)**	**MIU-2, 3 (40,41)**
Upper and Lower boundary of "Fracture zone along the fault"	—	**MIU-1, 2 and 3 (39～41)**

*：1: 25,000 "Toki" and "Mizunami" topographic maps published by Geophysical Survey Institute

Bolded: Data used to revise the initial, study area geological model

Uncertainties in the geological model are as follows.

① The MIU-1, 2 and 3 boreholes are nearly vertical. Therefore, steeply inclined fractures may be under-sampled.

② The methodology to specify permeable fractures needed to form an equivalent continuum model were not sufficiently established. As a result, the specification was unreliable.

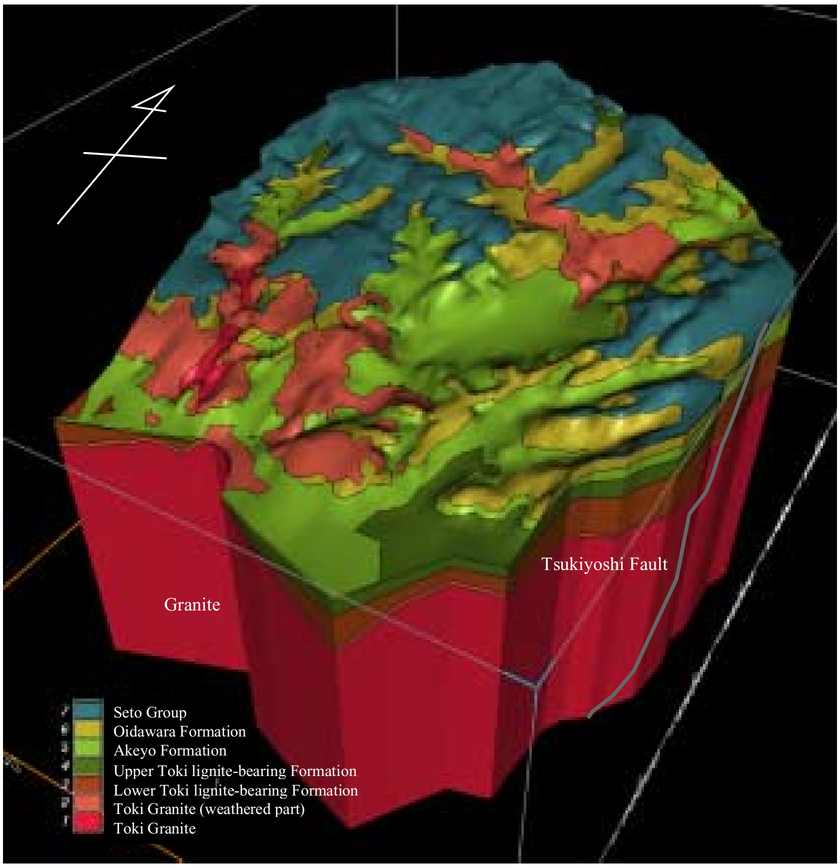

Figure 4.18 Geological model (about 4 km × about 6 km, down to 1,000m in depth) based on literature survey and existing data before the MIU Project

4.1.5 Construction of the geological model for the Shobasama Site

The model referred to here is the Shobasama Site-scale model. As was done for the other models, the procedure followed was to build the model iteratively starting with existing data and systematically adding information and knowledge to the model as new data became available.

4.1.5.1 Conceptualization of the geological model using data from literature survey and from other geoscientific research

The components of the Shobasama Site model may be divided into primary and secondary. In general the granite phases are primary whereas the structures such as fractures and weathered zones are secondary. Other structures such as the sedimentary rock layers are primary but with secondary structures such as crosscutting faults.

For the sedimentary rocks, the Seto Group, and the Oidawara, Akeyo and the Upper and Lower Toki Lignite-bearing Formations are the defined geological units (See Section 2.3). Though different lithofacies were recognized in the granite through the earlier investigations and analyses, enough information was not obtained for a reliable, deterministic modeling of their distribution and continuity. As for faulting, only the Tsukiyoshi Fault is considered to be well enough understood, and only in the sedimentary rocks, for inclusion in the model. Thus, this model is essentially the same as the initial model for the study area and is comprised of the same units in the granite:

① Fractured zone including the weathered zone,
② The granite below the weathered zone,
③ The Tsukiyoshi Fault.

The geological model of the Shobasama Site is shown in Figure 4.19. Three dimensional visualization software was not used because the software had not been introduced at the time and if it had would not likely have contributed meaningfully, as the model was too simple to benefit.

Uncertainties in the geological model are as follows.

① Knowledge of the subsurface distribution of geological units and the granite lithofacies were not well developed with the existing data base prior to 1996. As a result, the granite was only divided into two elements: the fractured zone including the weathered part and the rest of the granite.
② Information on the Tsukiyoshi Fault is not available in the granite. Thus, it is postulated that the fault in the granite has the same properties as that in the sedimentary rocks.

4.1.5.2 Revision of geological model using all data, including the results of MIU Phase I-a

Geological units

The general conceptualization developed for the first model of the sedimentary rocks remained basically unchanged. The units are divided into Seto Group, Oidawara Formation, Akeyo Formation, the Upper and Lower Toki Lignite-bearing Formation and Tsukiyoshi Fault. The MIU boreholes provided additional details on the layers in terms of thickness stratigraphy and confirmed the earlier findings.

Based on the borehole investigations in MIU-1, 2 and 3, the following improvements were possible.

① The secondary tectonic zones produced after the formation of the granite, the zone of weathering, the “Upper fracture zone”, “Moderately fractured zone”, the Tsukiyoshi Fault, and the “Fracture zone along the fault” were defined. Since the “Upper fracture zone” is thought to be characterized by a high fracture density and permeability, it could be distinguished from the “Moderately fractured zone” in the Biotite granite and Felsic granite. The Tsukiyoshi Fault has an approximately 100 m-wide fracture zone on both sides.

② Based on these results, the geological units established for the granite are the weathered part, the “Upper fracture zone”, the Tsukiyoshi Fault, “Fracture zone along the fault”, the Biotite granite and the Felsic granite.

Fracture zone distribution is shown schematically in Figure 4.20.

Model construction

Based on the data from the sources shown in Table 4.11, the boundaries of the geological units and the shape of the main fault plane were estimated using the minimum tension theory [(42)]. This model construction was carried out for the Shobasama Site, smaller than the above study area covers, and approximately 0.8 km×1.3 km, the “modeling area” (Figure 4.21). This modeling area contains the Tsukiyoshi Fault, which is presumed to greatly affect the hydrogeology of the Shobasama Site (See Section 4.2.4). Data sources used for the modeling are shown in Table 4.11. However, MIU-3 data was available too late for the modeling and therefore was not included in this exercise. Methods to establish the above-mentioned boundaries are as follows.

① Topographical surface:
Digital elevation data (Table 4.11) in 20 m intervals are used.

② Boundary between the Seto Group and the Oidawara Formation:
The Oidawara formation is restricted to the footwall (north side) of the Tsukiyoshi Fault, and therefore was not intersected by the boreholes drilled at the Shobasama Site. For modeling, the digitized contact shown on the geological map of the Toki-Mizunami district was used.

③ Boundary between the Seto Group and the Akeyo Formation:
This boundary is so shallow at the drilling sites in the Shobasama Site that no core was recovered. For the modeling, the digital information of the boundary location drawn on the geological map of the Toki-Mizunami district was used.

④ Boundary between the Akeyo and the Toki Lignite-bearing Formations:
The depth of this boundary was determined from the results of the MIU-1 and 2 borehole investigations. On the other hand, the Toki Lignite-bearing Formation is absent in the southern

part of the site and was not intersected by AN-1 or AN-3 nor is it visible in any surface exposure. Thus, on the knowledge that the unit does not extend to the south, depth information obtained in the MIU-1 and 2 are used for the modeling.

⑤ Boundary between the sedimentary rocks and the weathered part of the granite:

The MIU-1 and 2 and AN-1 and 3 borehole investigations established the depths of the boundary at the site. The upper part of the granite exposed on the ground surface is thought to be weathered. Accordingly, the depth information obtained in the boreholes and the digital database developed from the geological map of the Toki-Mizunami district are used for the modeling.

⑥ Boundary between the weathered granite and "Upper fracture zone" of the granite:

The weathered parts of the granite have the following characteristics.

· Zone with grade C_M or below by the rock mass rating in Japan [43]

· Zone dominated by RQD values of less than 50%

· Zone characterized by low resistivity or density and high porosity from geophysical logging

· Zone in the granite near the boundary with the sedimentary rocks. The matrix in this zone contains limonite and kaolinite [44], common weathering products.

Based on these definitions, the thickness of the weathered zone was estimated using data from MIU-1 and 2 and AN-1 and 3 borehole investigations.

⑦ Boundary between the "Upper fracture zone" and the "Moderately fractured zone" in the Biotite granite:

The "Upper fracture zone" is defined as a zone characterized by higher fracture density, higher porosity in geophysical logging and/or the frequent occurrence of horizontal fractures compared with the "Moderately fractured zone". This boundary is modeled using the information obtained from the MIU-1 and 2 borehole investigations.

⑧ Boundary between the "Moderately fractured zone" in the Felsic granite and the "Upper fracture zone"

This boundary is modeled using the information obtained from AN-1, 3 borehole investigations.

⑨ Boundary the "Moderately fractured zone" of the Biotite granite and the "Moderately fractured zone" of the Felsic granite

These are not distinguished on the existing geological map [12]. As a result, this boundary is modeled using the information obtained from the MIU-1, 2 and AN-1, 3 borehole investigations.

⑩ The Tsukiyoshi Fault

The Tsukiyoshi Fault was intersected by MIU-2, but not by the adjacent, more southerly MIU-1. Therefore, the depth information in MIU-2 and the digitized information of the fault line from the existing geological map [12] are input to the modeling. For modeling, 30 m of displacement by the Tsukiyoshi Fault was used (historic information) for the juxtaposition of units on opposite sides of the fault.

· Boundary between the Akeyo Formation and the Toki Lignite-bearing Formation

· Boundary between the sedimentary rocks and the underlying weathered granite

· Boundary between the weathered granite and the "Upper fracture zone"

· Boundary between the "Moderately fractured zone" in the Biotite and Felsic granites.

However, any genetic relationship between the "Upper fracture zone" and the Tsukiyoshi Fault is unknown. Therefore, the fault displacement of the boundaries between the "Upper fracture zone" and "Moderately fractured zone" in the Biotite granite and the Felsic granite were not considered.

⑪ Upper boundary of the "Fracture zone along the fault" (hanging wall side):
The information on thickness of the "Fracture zone along the fault" on the hanging wall side could only be obtained from MIU-2. Thus it has been assumed, for modeling, that the thickness of the fracture zone, as indicated by MIU-2, would be uniform all along the fault in the modeling area.

⑫ Lower boundary of the "Fracture zone along the fault" (footwall side):
The presence of the "Fracture zone along the fault" was confirmed on the footwall side of the Tsukiyoshi Fault in MIU-2. However, its lower boundary was not penetrated, so true thickness in unknown. Consequently, for lack of a better reason, the fractured zone on the footwall side of the fault is assigned the same thickness as on the hanging wall side.

Table 4.11 Data sources used to establish geological boundaries in the geological model

Boundary	Data	
	Literature study / geoscientific research except for the MIU Project	The result of MIU Phase I-a
Surface	Digital elevation data (20 m mesh)*	—
Upper boundary of Oidawara Fm.	Geological map (12)	—
Upper boundary of Akeyo Fm.	Geological map (12)	—
Upper boundary of Toki Lignite-bearing Fm. (Upper)	Geological map (12)	MIU-1, 2(39,40)
Upper boundary of weathered granite	Geological map (12) AN-1, 3 (34)	MIU-1, 2 (39,40)
Upper boundary of "Upper fracture zone"	AN-1, 3 (34)	MIU-1, 2 (39,40)
Upper boundary of "Moderately fractured zone" of the Biotite granite	—	MIU-1, 2 (39,40)
Upper boundary of "Moderately fractured zone" of the Felsic granite	AN-1, 3 (34)	—
Tsukiyoshi Fault	Geological map (12)	MIU-2 (40)
Upper/lower boundary of "Fracture zone along the fault"	—	MIU-2 (40)

* : 1: 25,000"Toki" and "Mizunami" topographic maps published by Geophysical Survey Institute

Uncertainties in the geological model are as follows.

① Data in the northeastern part of the Shobasama Site are lacking.
② Since the MIU-1, 2 and 3 boreholes are all vertical, information on fractures with a steep inclination is insufficient because they are statistically under sampled.
③ Information on the variation in thickness of the "Fracture zone along the fault" is insufficient.
④ Heterogeneity of the individual geological units of the granite are not known.
⑤ Information below 1,000 m depth is not available.

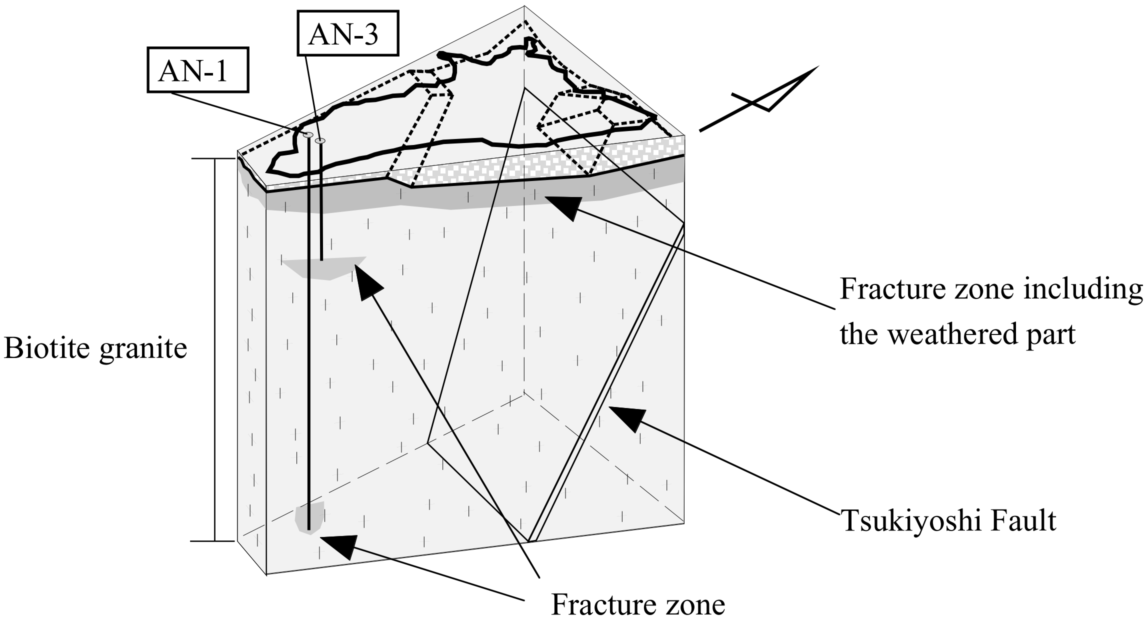

Figure 4.19 Geological model (Shobasama Site) based on literature survey and existing data before the MIU Project

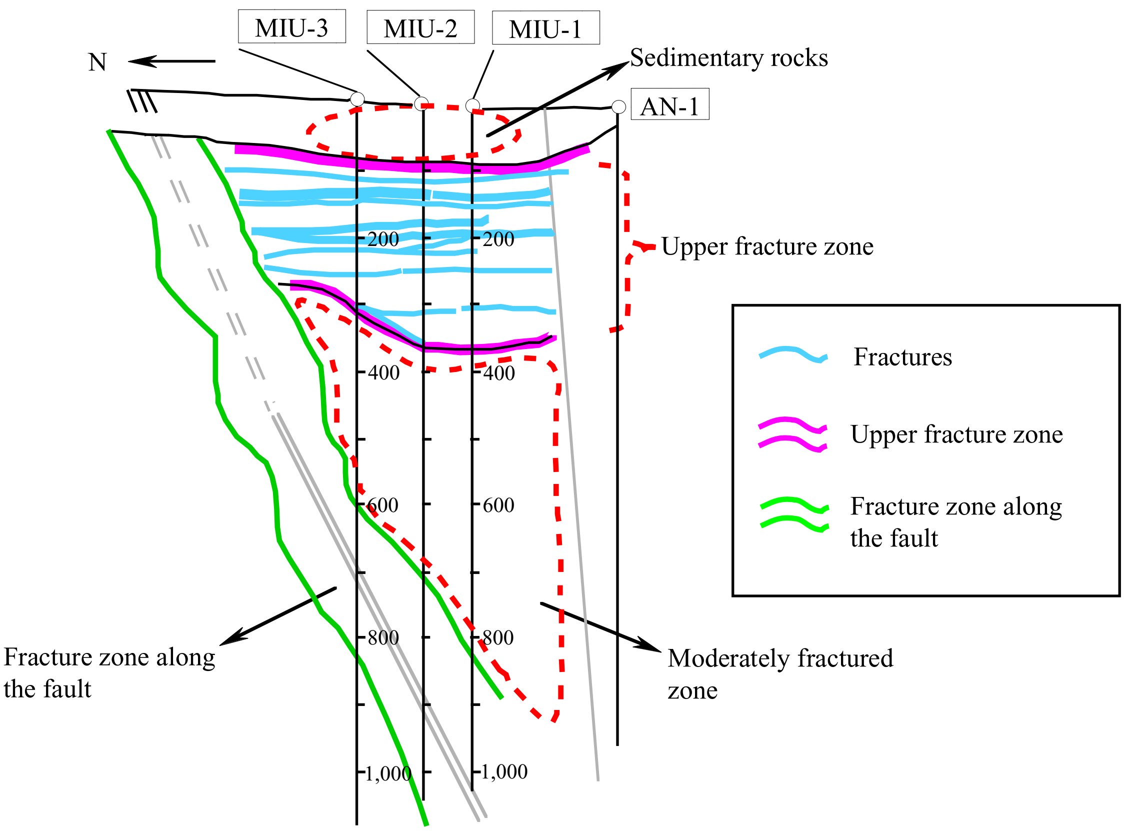

Figure 4.20 Distribution of fracture zone estimated with data from MIU-1~3

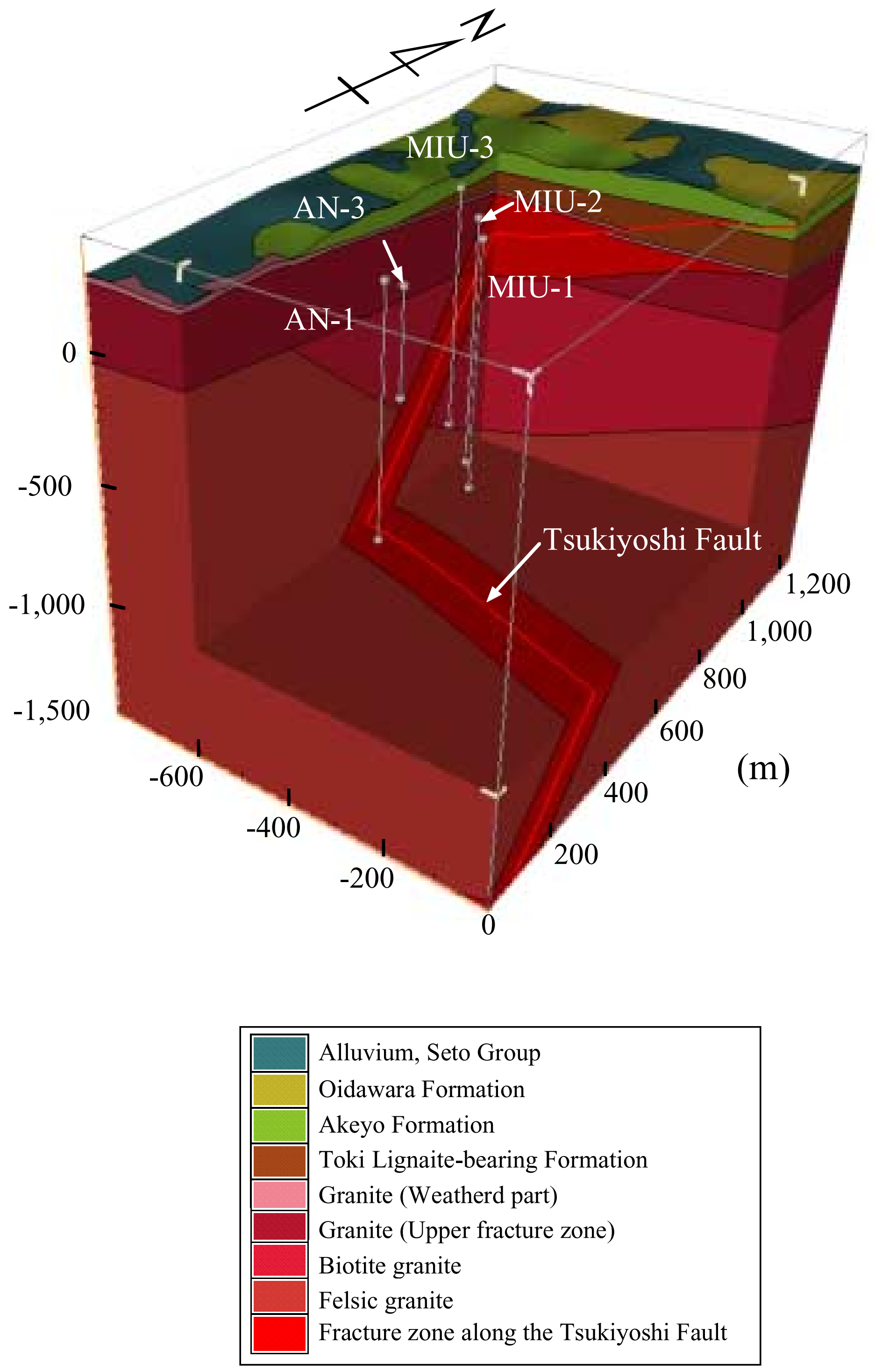

Figure 4.21 Geological model of the Shobasama Site based on the existing data and results of Phase I-a

4.1.6 Summary

The geological models are constructed so that the data requirements and the investigations performed in terms of the type, detail and scope and the analysis/evaluation techniques can be assessed in terms of their quality and accuracy. For each area, the Shobasama Site (0.8 km × 1.3 km) and the more regional study area for groundwater flow simulation (about 4 km×about 6 km), two increasingly detailed models were constructed. The first model for each of the above areas was based on the data from literature surveys and other geoscientific research. The second model was a revision of the first model, with new data from MIU Phase I-a investigations, including MIU-1, 2 and 3 boreholes.

In the first modeling exercise for both areas, the granite could only be divided into two parts, largely because of the lack of information regarding fracture zones in the granite and the possibility of variations in lithology. The two parts are the weathered zone at the top of granite and the remaining rock mass below the weathered zone.

In the second modeling exercise for both areas, new geological units defined in Phase I-a were added to the initial geological models. These units are the biotite granite, felsic granite, "Upper fracture zone", "Moderately fractured zone" and "Fracture zone along the fault". The revised models were utilized for construction of models for the other disciplines, namely the hydrogeological, hydrochemical and rock mechanical models and the numerical, groundwater flow simulation and rock response models. An important consideration in these exercises is knowing the data requirements of the models that build on the geological model.

The uncertainty in the revised geological models include the shortage of information on geological structures in the northeastern part of the Shobasama Site and at depths exceeding 1,000 m, little knowledge on the heterogeneities in the geological units defined and on the distribution of fractures with a steep inclination.

4.1.7 Future tasks

The future tasks are as follows:

① In order to improve the methodology of model construction, the uncertainty in the data and thus in the models should be investigated by comparing the existing models with new data and analysis in Phase I-b and later.

For example, geology and geological structure around the MIU-4 were predicted (Figures 4.22, 4.23) prior to drilling planned in Phase I-b. The predictions shown in Figures 4.22 and 4.23 were developed from the information presented in Figures 4.21 and 4.24 for each. Figure 4.24 [45] is a model constructed using all the available data prior to planning the MIU-4 drilling. Databases used for the construction of the geological models are shown in Table 4.12.

The revised geological models will be subject to evaluation by comparing predictions with the new information from the MIU-4 borehole investigations.

② The geological model constructed in Phase I-a was based on the assumption that the groundwater flow simulation will adopt a continuum modeling approach. Future groundwater flow simulations will likely adopt other modeling methodologies. It will be necessary to meet the data requirements of these methodologies with appropriate geological models.

③ Regional geological history should be understood as well as possible. If the geological model constructed in Phase I-a is not consistent with the geological history, the model should be revised to make it more reliable.

Table 4.12 Databases used to establish the geological boundaries in the geological model for planning MIU-4 borehole investigations

Boundary	Data source	
	Data obtained by literature study / Geoscientific research prior to MIU Project Phase I-a	The result of the Phase I-a
Ground surface	Digital elevation data (20 m mesh)*	—
Upper boundary of weathered granite	140 boreholes for uranium exploration AN-1, 3, 6 and 8, SN-1, 2, 3, 4 and 6, TH-1, 2, 3, 4, 5, 7 and 8, HN-1 Topographical map of basement rock (20,31) Seismic survey in the Shaft Excavation Effect Experiment	MIU-1, 2 and 3
Upper boundary of "Moderately fractured zone" in Biotite granite	AN-1, 3 (34)	MIU-1, 2 and 3
Upper boundary of "Moderately fractured zone" in Felsic granite	AN-1, 3 (34)	MIU-1, 2 and 3
Tsukiyoshi Fault	12 boreholes for uranium exploration TH-1, 2 and 3 Geological map (12)	MIU-2, 3

*: 1:25,000"Toki" and "Mizunami" topographic map published by Geophysical Survey Institute

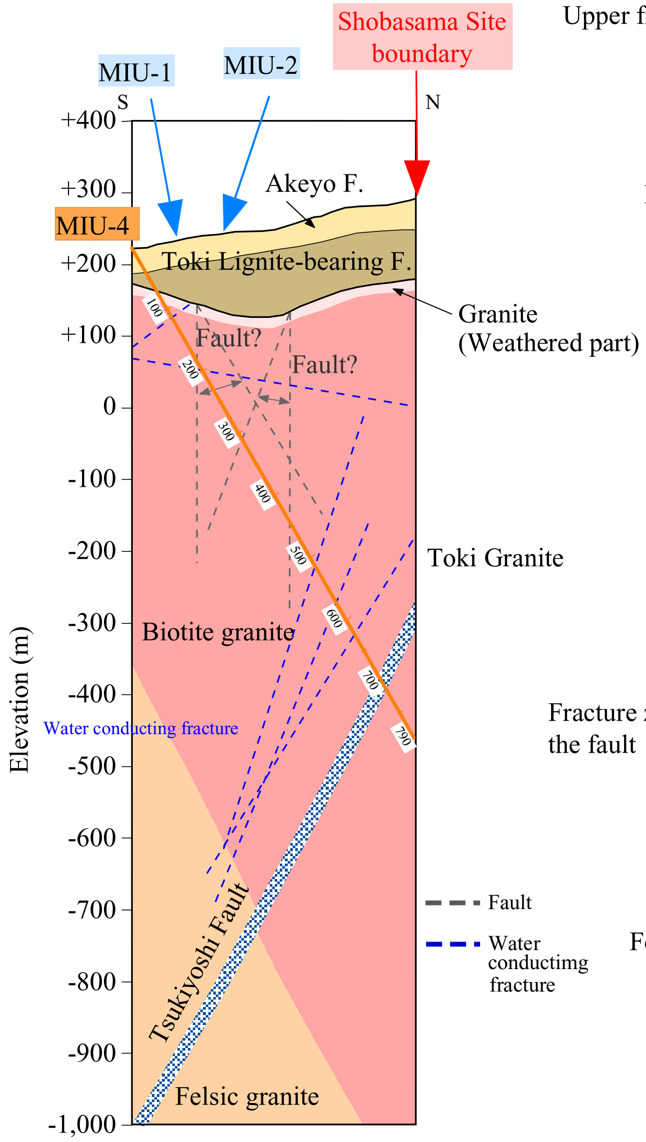

Figure 4.22 Cross section of geological model of the Shobasama Site based on the results of Phase I-a

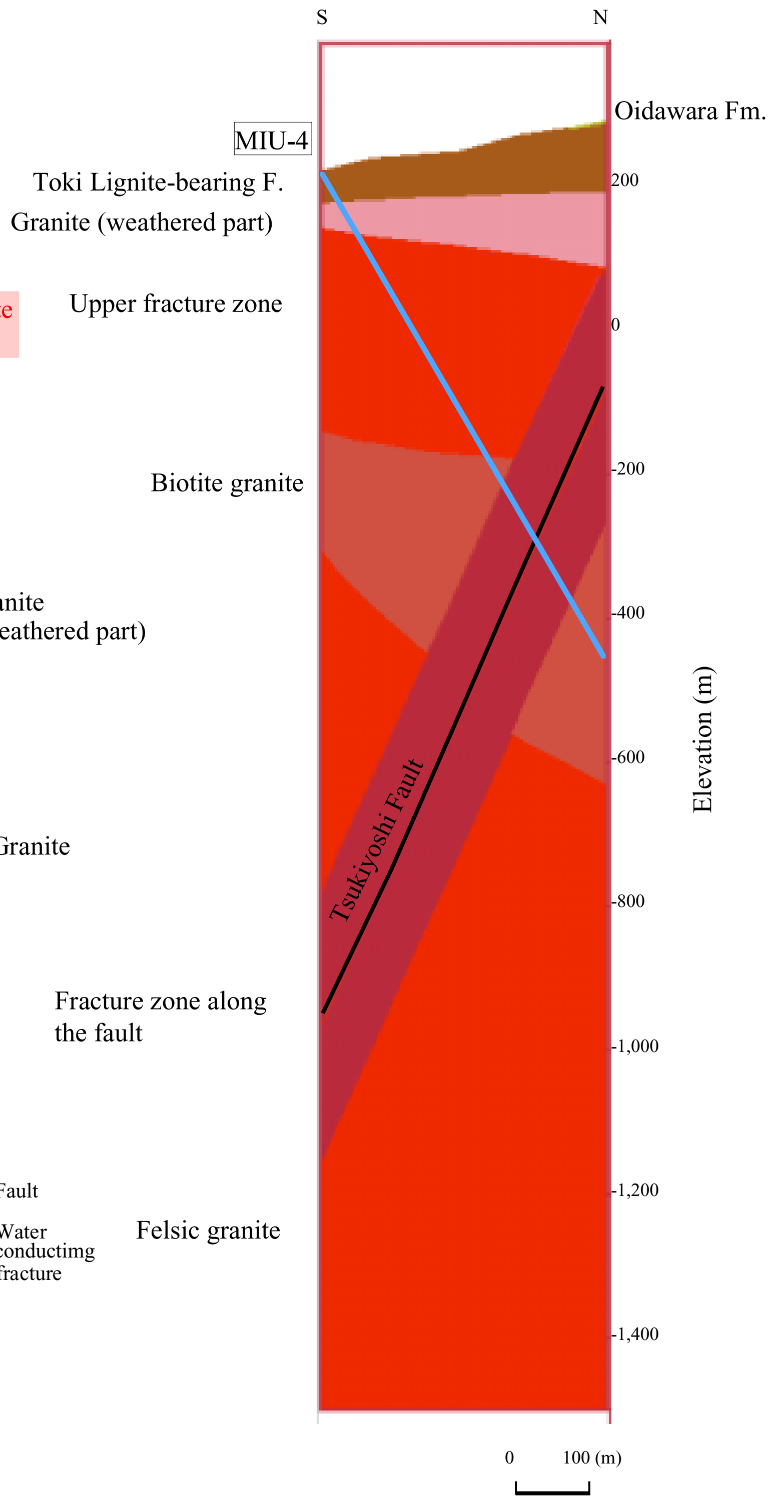

Figure 4.23 Cross section of geological model of the Shobasama Site (before MIU-4 excavation)

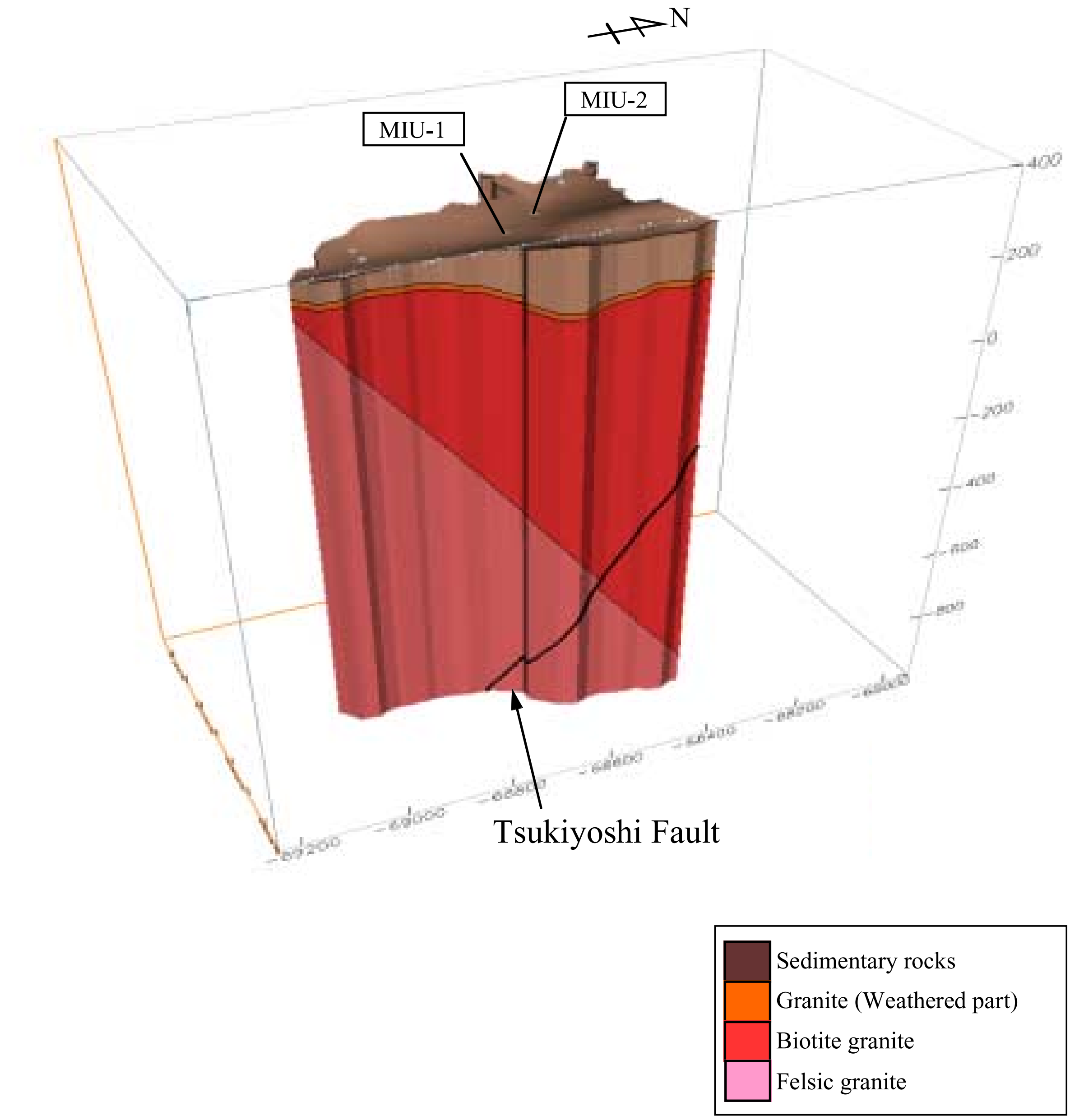

Figure 4.24 Geological model of the Shobasama Site (before MIU-4 excavation)